Cooperative Formation of Inorganic-Organic Interfaces in the Synthesis of Silicate Mesostructures

A. Monnier, F. Schuth, Q. Huo, D. Kumar, D. Margolese, R. S. Maxwell, G. D. Stucky, M. Krishnamurty, P. Petroff, A. Firouzi, M. Janicke, B. F. Chmelka

Science, New Series, Volume 261, Issue 5126 (Sep. 3, 1993), 1299-1303.

Cooperative Formation of Inorganic-Organic Interfaces in the Synthesis of Silicate Mesostructures

A. Monnier, F. Schüth, Q. Huo, D. Kumar, D. Margolese, R. S. Maxwell, G. D. Stucky,* M. Krishnamurty, P. Petroff, A. Firouzi, M. Janicke, B. F. Chmelka

A model is presented to explain the formation and morphologies of surfactant-silicate mesostructures. Three processes are identified: multidentate binding of silicate oligomers to the cationic surfactant, preferential silicate polymerization in the interface region, and charge density matching between the surfactant and the silicate. The model explains present experimental data, including the transformation between lamellar and hexagonal mesophases, and provides a guide for predicting conditions that favor the formation of lamellar, hexagonal, or cubic mesostructures. Model Q^{230} proposed by Mariani and his co-workers satisfactorily fits the x-ray data collected on the cubic mesostructure material. This model suggests that the silicate polymer forms a unique infinite silicate sheet sitting on the gyroid minimal surface and separating the surfactant molecules into two disconnected volumes.

The invention of a new family of mesoporous silica materials, designated M41S, by scientists at Mobil Oil Corporation (*1*), has dramatically expanded the range of crystallographically defined pore sizes from the micropore (<13 Å) to the mesopore (20 to 100 Å) regime. The synthesis uses ordered arrays of surfactant molecules as a "template" for the three-dimensional polymerization of silicates. The mesoporous materials obtained by this route exhibit several remarkable features: (i) well-defined pore sizes and shape, as compared to other mesoporous materials; (ii) fine adjustability of the pore size within the limits stated above; (iii) high thermal and hydrolytic stability if properly prepared; and (iv) a very high degree of pore ordering over micrometer length scales. These unusual properties are a direct result of the interplay between organized arrays of the surfactant molecules and silicate species in the aqueous phase.

Beck *et al.* (*2*) outlined two general pathways for the formation of the mesoporous silicates. The first model assumes that the primary structure-directing element is the water-surfactant liquid crystal phase. The second model suggests that the addition of the silicate orders the subsequent silicate-encased surfactant micelles. These general models, however, are insufficient for establishing the mechanistic understanding needed for better control of the synthesis process, which is key to efforts aimed at improving or adding to this exciting new class of materials. On the basis of experimental results, we present here a more detailed model of the mesophase formation process, which explains presently known experimental data and successfully predicts conditions needed for the synthesis of desired structures. We believe that this model can be generalized to the synthesis of other nonsiliceous materials as well.

From considerations in surfactant and silicate chemistry, three closely coupled phenomena are identified as crucial to the formation of surfactant-silicate mesophases. These include: (i) multidentate binding of silicate oligomers, (ii) preferred polymerization of silicates at the surfactant-silicate interface, and (iii) charge density matching across the interface.

Mesostructure syntheses can be carried out under conditions in which the silicate alone would not condense (at pHs from 12 to 14 and silicate concentrations of 0.5 to 5%) and the surfactant cetyltrimethylammonium (CTA^+) alone would not form a liquid crystal phase. In fact, surfactant-silicate mesophases can form at surfactant concentrations as low as 1%, a regime in the CTABr-water phase diagram in which only micelles are present. For a CTABr-water solution at typical surfactant-silicate synthesis temperatures in the absence of silicates, a hexagonal phase is favored at surfactant concentrations from ~25 to 70% by weight whereas a lamellar phase forms at concentrations above 70% (*3*, *4*). Nevertheless, a solid mesophase precipitate is formed, the structure of which will be discussed below, as soon as surfactant (chain length of 8 to 20 carbon atoms) and silicate solutions are combined. The rapidity of this precipitation indicates that there is a strong interaction between the cationic surfactant and anionic silicate species in the formation of surfactant-silicate mesophases.

We performed syntheses aimed at identifying conditions important for the formation of mesoporous materials over a wide range of reactant compositions and temperatures (*5*). For the purpose of investigation, we found that we could slow the evolution of the surfactant-silicate systems by undertaking the syntheses at moderate temperatures (between 30° and 100°C) (*6*). During freeze-dry kinetic experiments with CTACl used as the surfactant, a layered (lamellar) material with a primary *d* spacing (repeat distance) of 31(±1) Å was produced, together with amorphous silica, after reaction times on the order of 1 min. For the synthesis conditions given in Fig. 1, the lamellar mesophase disappears after approximately 20 min, at which point the diffraction pattern of the hexagonal mesostructure is simultaneously detected. This hexagonal material has a primary *d* spacing of 40(±1) Å and attains its final degree of ordering after ~10 hours (*7*).

A layered material with a primary *d* spacing of 31(±1) Å (Fig. 2, pattern A) can be isolated in pure form (*8*); a transmission electron microscopy (TEM) micrograph of this mesostructure is depicted in Fig. 3. The variation of the *d* spacing as a function of the chain length of a cationic surfactant $C_nH_{2n+1}[N(CH_3)_3]^+$ (for $14 \leq n \leq 22$) is 1.0 to 1.2 Å per carbon, which

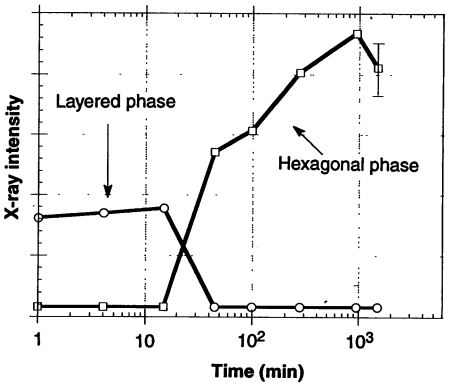

Fig. 1. Time evolution of the intensity of x-ray diffraction features associated with layered and hexagonal (M41S) mesostructures at 348 K. The layered material is precipitated rapidly, whereas the hexagonal material appears later, as a result of a higher degree of silica polymerization. The composition of the reaction mixture was as follows: 1 M SiO_2:0.025 M Al_2O_3:0.115 M Na_2O:0.233 M CTACl:0.089 M TMAOH:125 M H_2O.

A. Monnier, Department of Chemistry, University of California, Santa Barbara, CA 93106, and Departement de Chimie Physique Sciences II, 1211 Geneva, Switzerland.
F. Schüth, Department of Chemistry, University of California, Santa Barbara, CA 93106, and Institüt für Anorganische Chemie, Johannes-Gutenberg Universität, 6500 Mainz, Germany.
Q. Huo, D. Kumar, D. Margolese, R. S. Maxwell, G. D. Stucky, Department of Chemistry, University of California, Santa Barbara, CA 93106.
M. Krishnamurty and P. Petroff, Materials Department, University of California, Santa Barbara, CA 93106.
A. Firouzi, M. Janicke, B. F. Chmelka, Department of Chemical and Nuclear Engineering, University of California, Santa Barbara, CA 93106.
*To whom correspondence should be addressed.

corresponds to a monolayer assembly. If this new layered material is hydrothermally treated at 373 K (pH = 7), it is converted to the hexagonal mesostructure over 10 days, with intermediate and final x-ray patterns shown in Fig. 2, patterns B and C, respectively. During this transformation the degree of silica polymerization increases, as measured by the relative number of incompletely condensed (Q^3) and fully condensed (Q^4) silicon atoms determined by ^{29}Si magic-angle spinning nuclear magnetic resonance spectroscopy. The ratio between Q^3 and Q^4 silicon decreases from typical values of 1.0 for the layered material to 0.4 to 0.55 for the hexagonal mesostructure, reflecting a significant increase in the number of silicon atoms fully coordinated to other silicate nearest neighbors.

Mesophase formation and associated silica polymerization are intimately tied to Coulombic interactions between surfactant and silicate species at the micelle interfaces. Silicates present in the form of monovalent monomers, $Si(OH)_3O^-$, however, are expected to have little energetic advantage over other monovalent anions competing for access to the cationic surfactant head groups. At high pH, the reaction mixture also contains small silica oligomers (three to seven silicon atoms) of varying degrees of polymerization and charge (9). These oligomers are appreciably more acidic ($pK_a \sim 6.5$) than the monomer or dimer species [pK_a 9.8 and 10.7, respectively (*10*)], although all such silicates will be highly dissociated under the high pH conditions used here (*11*).

The oligomeric silica polyanions, however, can easily act as multidentate ligands for the cationic head groups of the surfactant, leading to a strongly interacting surfactant-silicate interface. Indeed, the interaction of ionic surfactants with polyions of opposite charge encourages strong cooperative binding, manifested by increases in the binding constants of up to two orders of magnitude in similar systems (*12*). Preferential multidentate binding of the silicate polyanions causes the interface to quickly become populated by tightly held silicate oligomers, which can subsequently polymerize further. Silicate polymerization within the surfactant-silicate interface region is favorable for two related reasons: (i) the concentration of silicate species near the interface is high and (ii) their negative charges are partially screened by the surfactant. Furthermore, as polymerization proceeds, the formation of highly connected silicate polyanions, which act as very large multidentate ligands, further enhances the cooperative binding between the surfactant and silicate species.

Multidentate ionic binding in surfactant-silicate systems has an important consequence; namely, it leads to precipitation of a given mesophase from solution. Through the interactions driving the precipitation process, the appearance of a given mesostructure is established, although this process is expected to operate on a different time scale from polymerization of the silica, which accounts ultimately for the thermal, mechanical, and hydrolitic stability of the final material. If small silica oligomers are present in sufficient quantity, precipitation of the surfactant-silicate system is primarily the result of electrostatic interactions, combined with packing constraints associated with the hydrophobic surfactant chains. Whereas precipitation is fast and essentially thermodynamically controlled, silica polymerization into a strong and extended framework is slow and reaction rate–limited. This two-stage process is in agreement with experimental findings that contrast the mesostructures obtained at room temperature after short reaction times with those obtained at high temperature after long reaction times: very similar x-ray patterns are obtained for both sets of conditions, indicating identical precipitated mesostructures; however, the materials synthesized by the low-temperature route are thermally and mechanically much less stable than the high-temperature analogs. The coupling between the precipitation and polymerization processes in surfactant-silicate systems provides the basis for the lamellar-to-hexagonal mesophase transformation in a way that we now describe.

The resemblance, in shape and size, of the surfactant-silicate mesostructures with the corresponding water-surfactant liquid crystal phases indicates that the interactions responsible for these morphologies are of a similar nature. The governing role of the head-group area (A) in the selection of a particular mesophase has already been recognized in water-surfactant systems: the favored mesophase is that which permits A to be closest to its optimal value A_0, while maintaining favorable packing of the hydrophobic surfactant chains (*13*). In surfactant-silicate systems, the value of A_0 is strongly affected by electrostatic and steric interactions between the silicate and surfactant micelle species. More quantitatively, its value is obtained by minimizing the Gibbs free energy G as a function of A:

$$A_0 \rightarrow (\partial G/\partial A) = 0 \quad (1)$$

$$G(A,\rho) = G_{intra}(A) + G_{wall}(\rho) + G_{inter}(A, \rho) + G_{sol} \quad (2)$$

where G_{intra} reflects the van der Waals forces and conformational energy of the hydrocarbon chains and the van der Waals and electrostatic interactions of the head group within a single micelle; G_{wall} accounts for the polysilicate structural free energy, including the solvent, counterion, and silicate van der Waals and electrostatic interactions within the inorganic silicate framework or "wall"; G_{inter} reflects the van der Waals and electrostatic effects associated with wall-micelle and micelle-micelle interactions; G_{sol} describes the solution phase; and ρ specifies the compositions of the various species within the wall. The chemical potentials of these species are set by the concentration of the corresponding species in the aqueous solution, as accounted for by G_{sol}.

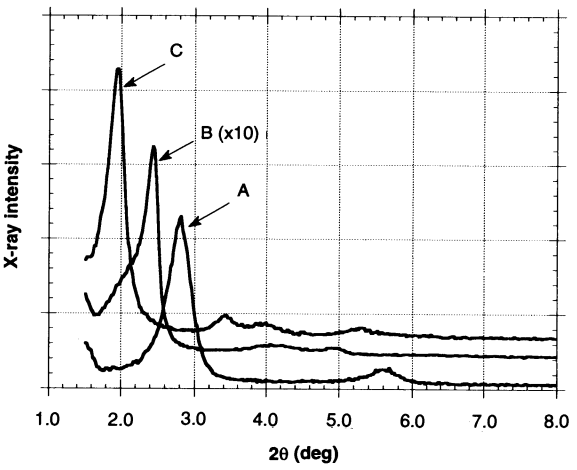

Fig. 2. Powder x-ray diffraction patterns of surfactant-silicate mesostructures precipitated from the same reaction mixture (1 M SiO_2: 0.034 M Al_2O_3:0.07 M Na_2O:0.27 M CTABr:0.14 M TMAOH:0.28 M TMB:100 M H_2O), and then treated hydrothermally at 373 K for different times. X-ray patterns are shown for (curve A) the initially precipitated layered material, (curve B) an intermediate material, and (curve C) the M41S hexagonal mesostructure acquired 0, 1, and 10 days, respectively, after initiation of the hydrothermal treatment.

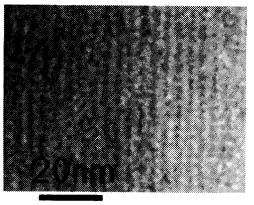

Fig. 3. Transmission electron micrograph of the layered surfactant-silicate mesostructure whose x-ray data are shown in Figs. 1 and 2 (curve A). The *d* spacing of this material is 31(±1) Å.

Physically, G_{intra} governs the formation of a particular micelle shape for a given value of A and is also responsible for the observed swelling of the micelles when hydrocarbon "expanders," such as trimethylbenzene (TMB) are added to the solution (*14*). The term G_{wall} drives the chemistry within the wall, including the polymerization process, and contains the structural constraints responsible for the multidentate binding. The term G_{inter} establishes the relation between A and the state of the wall described by ρ. This coupling across the interface can be understood in terms of electrostatic interactions (which most likely predominate), whereby the silicate charge density within the wall, ρ_ϵ, is mutually screened by the charges on the surfactant head groups, which have an average surface charge density of 1/A. Thus, the electrostatic interactions link A_0, as defined by Eq. 1, with ρ_ϵ, a relation we refer to as "charge density matching." Such interdependent electrostatic effects control the *d* spacings of surfactant intercalates in different mica-type silicates (*15*) and have been invoked to explain the "self-replication" process of silica layers in purely inorganic systems (*16*).

In surfactant-silicate systems, polymerization driven by G_{wall} will profoundly affect ρ_ϵ, providing a mechanism to explain the transition between the lamellar and hexagonal mesophases. In the early stage of the synthesis, the presence of highly charged silica oligomers favors a small value of A_0, which can be achieved with a lamellar surfactant configuration. As rearrangement and polymerization of the silicate species proceed, the density of anionic silanol groups diminishes, so that A_0 increases, while the number of compensating cations decreases. At the same time, the wall thickness can decrease from its initial value without energy cost, because the most stable ionized silanol groups are confined to the wall surface, thus reducing repulsive dipole-dipole interactions between the two opposite-facing wall surfaces. The silicate wall is still poorly condensed during early stages of the synthesis, allowing the system to increase its A toward A_0 by adopting the hexagonal structure according to charge-density matching criteria. Under these circumstances, the wall thickness simultaneously decreases to keep the volume ratio CTA/SiO_2 constant. The actual wall thickness has been estimated to be 10 to 11 Å (*17*) for the lamellar mesophase and 8 to 9 Å (*18*) for the hexagonal mesophase. Simple geometrical arguments can be used to show that these values are consistent with a constant CTA/SiO_2 volume ratio throughout the phase transition.

The regularity of the product mesostructures supports mediation of the silicate wall thickness during the assembly process. The high efficiency of this mediation is reflected by the experimental observation that the wall thickness of the hexagonal phase is essentially constant (8 to 9 Å) over a wide range of reaction conditions, independent of the surfactant chain length, and by the clearly hexagonal, as opposed to circular, pore shape established by both high-resolution TEM and modeling of the powder x-ray diffraction patterns (*19*). Control of the silicate wall thickness is undoubtedly related to the double layer potential: silicate species are only accumulated at the surfactant interface to the extent necessary for charge compensation. Polymerization normal to the interface, which would thicken the wall or produce amorphous bulk SiO_2, does not occur because of the strong electrostatic repulsion produced by the high negative charge on the silicate species at pH 12 and above (*10*).

Figure 4 shows a mechanism consistent with current experimental investigations by which the lamellar-to-hexagonal mesophase transformation may occur. Silica polymerization leads to an increase in interfacial area that is achieved through corrugation of the lamellar surfactant-silicate sheets. As implied in the final step, this corrugation progresses until connection between the sheets is made at the cusps, resulting ultimately in the formation of the hexagonal mesophase. Another way to accommodate the change in A would be to maintain a planar structure while tilting the hydrocarbon chains. Such a transition, however, is entropically disfavored by the restrictive chain configuration this suggests.

Yanagisawa *et al.* (*20*) recently reported a hexagonal mesostructure, with pore dimensions similar to that of M41S, produced by the inclusion of CTA^+ cations into the sheet silicate kanemite. During their synthesis these researchers observed a layered intermediate that subsequently transformed into a hexagonal phase material. This process is probably driven by the same forces as the transformation we report, although it is not yet clear to what extent the kanemite structure is preserved during the conversion. If the pH is sufficiently basic, for example, the sheets can be partially or fully destroyed during the process.

We propose that the surfactant-silicate mesophase structure is governed primarily by the terms G_{intra} and G_{inter} of Eq. 2. In this respect, the main effect of the silicate wall and of the reaction conditions are to determine A_0. This provides predictive capability for establishing the reaction conditions that favor the lamellar or the hexagonal mesophases. We have tested this model experimentally by monitoring the effects of pH and the degree of polymerization of the silica source on the mesostructure syntheses, with the results summarized in Fig.

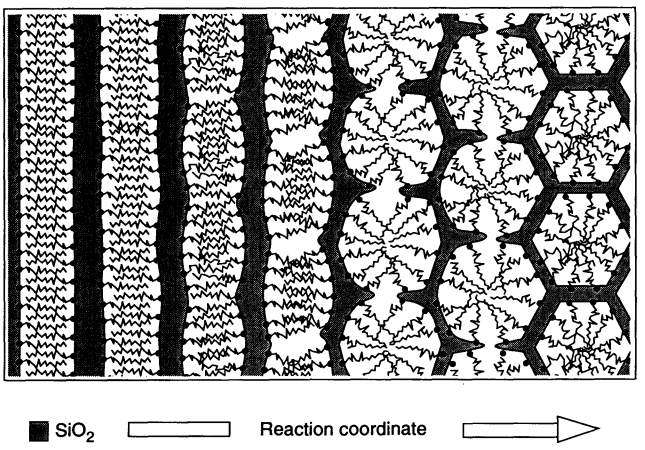

Fig. 4. Schematic diagram of the mechanism proposed for the transformation of a surfactant-silicate system from the lamellar to the hexagonal mesophase. On the left, small silica oligomers (not shown explicitly in the gray SiO_2 region) act as multidentate ligands, which have sufficiently high charge density to permit a lamellar surfactant configuration. As polymerization of the silica proceeds, diminished charge density of larger silica polyanions increases the average head-group area of the surfactant assembly, driving the transformation into the hexagonal mesophase.

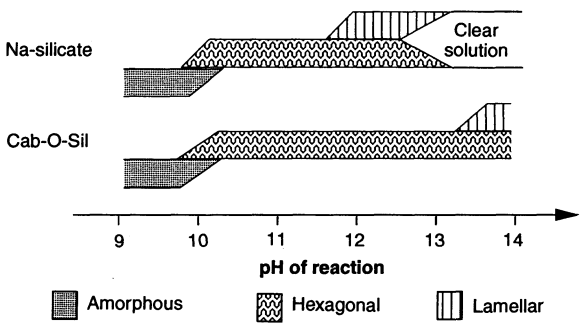

Fig. 5. Chart showing the approximate domains of formation of the lamellar and hexagonal surfactant-silicate mesophases, as functions of pH and silica source. Cab-O-Sil is composed of ~100 Å oligomeric silica particles, whereas Na-silicate is a solution of hydrolyzed and essentially monomeric silicates.

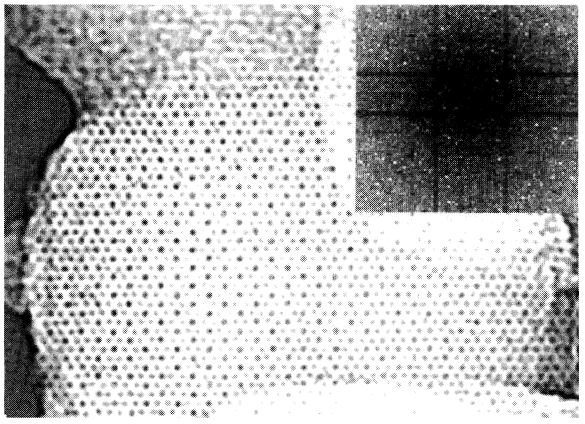

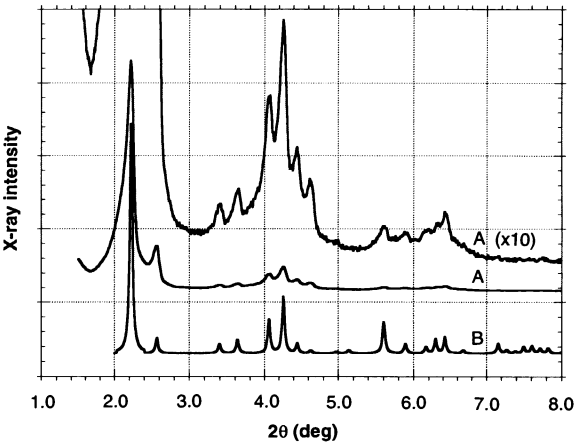

Fig. 6 (left). Transmission electron micrograph of the cubic surfactant-silicate mesostructure showing an ordered ~2000 Å aggregate viewed along its [111] axis. **Fig. 7 (right).** X-ray powder diffraction pattern of the cubic mesostructure, with $Ia\bar{3}d$ symmetry, synthesized from a reaction mixture with a molar composition of 1 M TEOS:0.25 M Na_2O:0.65 M CTACl:62 M H_2O for 3 days at 373 K (curve A). Calculated diffraction pattern using the Q^{230} model proposed by Mariani *et al.* (*21*) with a lattice parameter a = 97.3 Å (curve B).

5. These results lead to the following conclusions in accordance with our predictions:

1) The lamellar phase is favored at high pH and for a low degree of polymerization of the silica source.

2) The hexagonal phase is favored at low pH and for a highly polymerized silica source.

In addition, we investigated the influence of the ionic strength on the surfactant-silicate assembly process by performing the synthesis in a reaction solution also containing 1 M NaCl. The presence of the salt decreased the regularity of the material, as reflected by a reduction in the number of peaks in the x-ray pattern (from four to two). This effect, expected only at high ionic strengths, is attributed to perturbation of the double layer potential. The strong binding constant of silicate species compared to other ions makes this effect negligible at lower ionic strengths and explains why mesostructure syntheses are relatively insensitive to other counterions in the reaction mixture.

The existence of the cubic mesophase described by Beck *et al.* (*2*) is strongly supportive of the important role of $G_{intra} + G_{inter}$ in the formation of surfactant-silicate mesostructures. Indeed, there is remarkable similarity between the cubic mesophase, which we have recently synthesized and characterized, and the $Ia\bar{3}d$ phase found in the water-CTABr system (*4*). A TEM image of the cubic mesostructure material (Fig. 6) shows an ordered ~2000 Å aggregate. The x-ray powder spectrum (Fig. 7) agrees very well with the model Q^{230} proposed by Mariani *et al.* (*21*) for water-surfactant systems. For this structure, it is appealing to conjecture that the midplane of the silicate wall sits on a gyroid periodic minimal surface (*22*). Such a structure can then be viewed as a single infinite silicate sheet that separates the surfactant species into two equal and disconnected volumes. This so-called bicontinuous phase will be formed when the value of A_0 set by the reaction conditions is close to the value of the $Ia\bar{3}d$ phase, namely, when pH and the CTA/SiO_2 ratio are high. It is advantageous for the silicate wall to occupy a periodic minimal surface, because it can maximize the wall thickness for a given CTA/SiO_2 volume fraction.

The leading role of $G_{intra} + G_{inter}$ in directing mesostructure formation provides a foundation for identifying potential replacement candidates for silicon in the synthesis of mesoporous inorganic frameworks. The principal criteria are that the inorganic component must be capable of forming flexible polyionic species, that extensive polymerization of the inorganic component must be possible, and that charge density matching between the surfactant and inorganic species has to occur. In other words, when G_{sol} plays a benign role, G_{wall} must not dominate $G_{intra} + G_{inter}$ in order that the mesostructure form.

In addition to binding efficiently to the surfactant interface, the best inorganic candidates will have a tendency to form glasses easily. Silicates are certainly a prototypic system in view of the ease with which they form oligomeric anions with varying degrees of polymerization. Other systems, however, may also fulfill these requirements, including transition metals, such as vanadium, or main group elements, such as boron, which can form polyanions and condense. One can also speculate about a reversed system in which an anionic surfactant is used to precipitate a cationic metal oxide precursor, the laurylsulfate–iron oxide system representing one candidate example.

Existing experimental data thus far confirm the trends predicted for the formation of surfactant-silicate mesostructures by the qualitative model outlined above. Cooperative binding provides an explanation for the strong interactions needed to precipitate mesophases from dilute solutions. Preferential polymerization of silicates in the region of the interface together with a double layer control of the wall thickness are responsible for the high regularity of the surfactant-silicate mesostructures. Charge density matching establishes a link between the chemical composition and structure of the silicate wall and the formation of a particular mesostructure. We expect that these perspectives will stimulate and guide experiments aimed at producing and exploiting a better understanding of this exciting class of materials.

REFERENCES AND NOTES

1. C. T. Kresge, M. E. Leonowicz, W. J. Roth, J. C. Vartuli, J. S. Beck, *Nature* **359**, 710 (1992).
2. J. S. Beck *et al.*, *J. Am. Chem. Soc.* **114**, 10834 (1992).
3. R. G. Laughlin, *Surfactant Sci. Ser.* **37**, 1 (1991).
4. X. Auvray, C. Petipas, R. Anthore, I. Rico, A. Lattes, *J. Phys. Chem.* **93**, 7458 (1989).
5. The general procedure for synthesizing mesostructure materials is as follows: An aqueous solution containing silica and optional tetramethylammonium hydroxide (TMAOH) is stirred into an aqueous solution containing the surfactant and an optional aluminum source. The resulting mixture is kept at temperatures between 298 and 423 K for reaction times between 5 min and 3 days in either closed Teflon bottles or under stirring and refluxing in a glass flask. For silica sources, we used Cab-O-Sil M-5 (Kodak, Rochester, NY), an aqueous solution of sodium silicate (27.5% SiO_2, SiO_2/Na_2O = 3.22 from PQ Corporation, Valley Forge, PA), or tetraethylorthosilicate (TEOS) (Aldrich, Milwaukee, WI). Aluminum sources were boehmite (CATAPAL B from Alumina Vista, Houston, TX) or sodium aluminate (Spectrum Chemical, Gardena, CA). Quaternary ammonium alkyls $C_nH_{2n+1}(CH_3)_3NX$, where X = Cl^- or Br^- and n = 8 to 18, and TMAOH were obtained from Aldrich.

6. The expression "surfactant-silicate" is used here as a comprehensive term for materials synthesized using a mixture of surfactant and silica species, regardless of the particular structure.
7. The transformation between the lamellar and hexagonal mesophases was observed after freeze-drying, as well as air-drying, the filtered samples.
8. Addition of trimethylbenzene (TMB) to the reaction mixture stabilizes the lamellar mesophase. Experiments have shown that the 31(±1) Å repeat distance for the layered material shown in Figs. 2A and 3 is preserved over a range of TMB concentrations between 0.5 and 3.0 M, whereas at lower TMB concentrations the hexagonal mesostructure is the favored product. Stabilization of the lamellar mesophase likely occurs because TMB dissolved within the surfactant hydrocarbon assemblies contributes to the hydrophobic chain volume. This increase in surfactant chain volume increases the value of A_0 at which the lamellar-to-hexagonal mesophase transformation occurs, according to a simple geometric model (*13*). Thus, the mesostructural transformation depicted in Fig. 2 is a consequence of hydrothermal removal of TMB from within the surfactant chain assembly, combined with an increase in A_0. This conclusion is supported by separate experiments which show that addition of TMB to the aqueous phase inhibits the transformation from a lamellar to a hexagonal mesostructure.
9. R. K. Harris, C. T. G. Knight, W. E. Hull, *ACS Symp. Ser.* **194**, 79 (1982); C. T. G. Knight, R. G. Kirkpatrick, E. Oldfield, *J. Magn. Reson.* **78**, (1988); A. V. McCormick and A. T. Bell, *Catal. Rev. Sci. Eng.* **31**, 97 (1989).
10. R. K. Iler, *The Chemistry of Silica* (Wiley, New York, 1979), p. 182.
11. C. J. Brinker, G. W. Scherer, *Sol-Gel Science* (Academic Press, New York, 1990), p. 100.
12. K. Hagakawa and J. C. T. Kwac, *Surfactant Sci. Ser.* **37**, 189 (1991).
13. J. Charvolin and J. F. Sadoc, *J. Phys.* **48**, 1559 (1987). J. N. Israelachvili [in *Surfactants in Solution*, K. L. Mittal and P. Bothorel, Eds. (Plenum, New York, 1987), vol. 4, p. 3] proposed the dimensionless parameter $g = V/A_0\ell_c$ as a means of determining the preferred configuration of a surfactant assembly, where V is the volume of the hydrophobic chain and ℓ_c is the characteristic chain length. According to this treatment, spherical micelles will form if $g < 1/3$, cylindrical micelles if $1/3 < g < 1/2$, vesicles or bilayers if $1/2 < g < 1$, and inverted micelles if $g > 1$.
14. As discussed in (*7*), the presence of TMB in the reaction mixture can, but does not always, require a swelling response in surfactant systems.
15. A. Weiss, *Clays and Clay Minerals. Proceedings of the National Conference on Clays and Clay Minerals* (Earl Ingerso, New York, 1961), vol. 10, p. 191.
16. A. Weiss, *Angew. Chem. Int. Ed. Engl.* **20**, 850 (1981).
17. The hexagonal shape of the mesopores can be determined from the y intercept of a plot of d spacings versus the number of carbon atoms for different chain length surfactants, corrected for the head-group diameter.
18. Calculated from d spacings, volumetric considerations (based on a measured void fraction of 0.65), and x-ray diffraction refinements based on the use of cylinder- and hexagonal-prismatic-rod-packing as models.
19. A. Monnier and G. D. Stucky, unpublished work.
20. T. Yanagisawa, T. Shimizu, K. Kuroda, C. Kato, *Bull. Chem. Soc. Jpn.* **63**, 988 (1990).
21. P. Mariani, V. Luzzati, H. Delacroix, *J. Mol. Biol.* **204**, 165 (1988).
22. A periodic minimal surface is the smallest surface separating a volume into two equal parts, given a certain periodic constraint.

23. We thank J. Israelachvili, J. Zasadzinski (UCSB), C. Kresge, D. Olson, J. Beck, J. Vartuli, and J. Higgins (Mobil) for helpful discussions. This research was funded by Air Products, du Pont, the MRL Program of the National Science Foundation under award DMR 9123048, the Office of Naval Research (G.D.S.), the NSF Science and Technology Center for Quantized Electronic Structures (grant DMR91-20007), the NSF/NYI program, and the Camille and Henry Dreyfus Foundation (B.F.C.) and through fellowships by the FNRS (A.M.) and the DFG (F.S.).

26 April 1993; accepted 8 July 1993

An Unnatural Biopolymer

Charles Y. Cho, Edmund J. Moran,* Sara R. Cherry, James C. Stephans, Stephen P. A. Fodor, Cynthia L. Adams, Arathi Sundaram, Jeffrey W. Jacobs, Peter G. Schultz†

A highly efficient method has been developed for the solid-phase synthesis of an "unnatural biopolymer" consisting of chiral aminocarbonate monomers linked via a carbamate backbone. Oligocarbamates were synthesized from *N*-protected *p*-nitrophenyl carbonate monomers, substituted with a variety of side chains, with greater than 99 percent overall coupling efficiencies per step. A spatially defined library of oligocarbamates was generated by using photochemical methods and screened for binding affinity to a monoclonal antibody. A number of high-affinity ligands were then synthesized and analyzed in solution with respect to their inhibition concentration values, water/octanol partitioning coefficients, and proteolytic stability. These and other unnatural polymers may provide new frameworks for drug development and for testing theories of protein and peptide folding and structure.

Polypeptides have been the focus of considerable attention with respect to their structure and folding, biological function, and therapeutic potential. The development of efficient solid-phase methodology for the synthesis of peptides (*1*), peptide derivatives (*2*), and large peptide libraries (*3–8*) has greatly facilitated these studies. The development of efficient methods for the synthesis of unnatural biopolymers (*9–11*) composed of building blocks other than amino acids may provide new frameworks for generating macromolecules with novel properties. For example, polymers with improved pharmacokinetic properties (such as membrane permeability and biological stability) might facilitate drug discovery, and polymers with altered conformational or hydrogen-bonding properties may provide increased insight into biomolecular structure and folding. We report the highly efficient solid-phase synthesis of oligocarbamate polymers from a pool of chiral aminocarbonates and the synthesis and screening of a library of oligocarbamates for their ability to bind a monoclonal antibody (mAb).

The oligocarbamate backbone (Fig. 1), in contrast to that of peptides, consists of a chiral ethylene backbone linked through relatively rigid carbamate groups. The α carbon, like that of peptides, is substituted with side chains that contain a variety of functional groups. Although the β carbon is unsubstituted in our initial target, additional backbone modifications (and conformational restriction) can be incorporated via alkylation of the β carbon or the carbamyl nitrogen. Oligocarbamates were synthesized from a pool of optically active *N*-protected aminocarbonates (Fig. 2) which, in turn, were derived from the corresponding optically active amino alcohols. The latter are either commercially available or can be prepared in chiral form by reduction of the *N*-hydroxysuccinimidyl or pentafluorophenyl esters of *N*-protected amino acids (*12*). The α-amino group was protected with the use of either nitroveratryl chloroformate (*13*) (NVOC-Cl) (for photochemical deprotection) or fluorenylmethyl-*N*-hydroxysuccinimidyl carbonate (Fmoc-OSu) (for base-catalyzed deprotection) (*14*). When necessary, side chains were protected as acid-labile *tert*-butyl esters, ethers, or carbamates. Protected amino alcohols were converted to the corresponding *N*-protected *p*-nitrophenyl carbonate monomers by reaction with *p*-nitrophenyl chloroformate in pyridine/CH_2Cl_2, generally in >80% yield. The carbonate monomers are stable for months at room temperature.

Solid-phase synthesis of oligocarbamates involves the sequential base-catalyzed or light-dependent deprotection of the α-amino group of the growing polymer chain followed by coupling to the next protected *p*-nitrophenyl carbonate monomer (Fig. 2). The *N*-protected "hydroxy-terminal" residue was covalently attached to polystyrene resin containing either *N*-protected *p*-alkoxybenzyl amino

C. Y. Cho, E. J. Moran, S. R. Cherry, J. C. Stephans, P. G. Schultz, Department of Chemistry, University of California, Berkeley, Berkeley, CA 94720.
S. P. A. Fodor, C. L. Adams, A. Sundaram, J. W. Jacobs, Affymax Research Institute, 4001 Miranda Avenue, Palo Alto, CA 94304.

*Present address: Ontogen Corporation, 2325 Camino Vida Roble, Carlsbad, CA 92009.
†To whom correspondence should be addressed.